Reaction Kinetics, Mechanisms and Catalysis (2023) 136:107–124
https://doi.org/10.1007/s11144-023-02349-4

Converting glycerol into glycerol carbonate by transesterification with different esters: reaction steps and coproducts

Gustavo Medeiros de Paula[1] · Janaina Guedes Eid[1] · Dilson Cardoso[1]

Received: 14 November 2022 / Accepted: 8 January 2023 / Published online: 28 January 2023

Abstract

Glycerol carbonate was produced by transesterification between glycerol and different esters (dimethyl carbonate, diethyl carbonate, ethylene carbonate and propylene carbonate), using CTA-MCM-41 hybrid silica as basic catalyst. CTA-MCM-41 hybrid silica was synthesized using a non-hydrothermal method and was characterized by X-ray diffraction, thermogravimetric analysis and scanning electron microscopy. The catalyst characterizations showed that it had a hexagonal structure, catalytic sites concentration of 1.822 mmol g^{-1} and particle size in the range of 1–5 μm. The reactions for formation of glycerol carbonate were performed in a batch reactor, with dimethylformamide as solvent, and the products were analyzed by gas chromatography (GC-FID) and (GC–MS). Experiments were performed to study the effects of ester, temperature, catalyst percentage, and molar ratio of the reactants. The main products of the reactions with these esters were glycerol carbonate, glycidol and small amounts of glycerol monocarbonates, glycerol tricarbonate and glycidol carbonate. Cyclic-chain esters showed greater reactivity than straight-chain esters, forming fewer co-products. The reactions with straight-chain esters presented seven reaction steps, three more than the reactions with cyclic-chain esters. Straight-chain and cyclic-chain esters formed the products and co-products following different reaction mechanisms.

Keywords CTA-MCM-41 hybrid silica · Glycerol · Glycerol carbonate · Glycidol · Reaction mechanism

✉ Dilson Cardoso
dilson@ufscar.br

[1] Catalysis Laboratory, Department of Chemical Engineering, Federal University of São Carlos, Rod. Washington Luiz, km 235, São Carlos, SP 13565-905, Brazil

Introduction

The industrial production of biodiesel has expanded in recent decades and now accounts for a large part of the renewable diesel market, especially in countries such as the United States, Brazil, Indonesia, and Germany. The manufacture of this biofuel generates large volumes of glycerol, the main co-product, in a proportion of 8–10%, relative to the volume of biodiesel [1–3]. For example, in 2021, Brazil produced about 6.77 million m^3 of biodiesel (B100) and 613 thousand m^3 of glycerol [4]. Most of the applications for glycerol are found in the pharmaceutical and food industries. However, the expansion of the biodiesel industry has broadened the horizons for the use of this co-product as raw material in the manufacture of other valuable products in the chemical industry [2, 5, 6]. Notably, glycerol carbonate has become an industrially promising molecule, since it is derived from biomass and has several direct and indirect applications, including as a solvent or co-solvent [7], a building block in polymer manufacture [8], and a fuel additive [9].

Glycerol carbonate can be obtained using processes such as carbonation, transcarbonation, transesterification, and glycerolysis [10, 11]. Specifically, the transesterification between glycerol and dimethyl carbonate has been viewed as the simplest and greenest process [11, 12]. Nonetheless, despite being considered a simple process, the production of glycerol carbonate by transesterification is complex and, although dimethyl carbonate (DMC) is the most common reagent, other carbonic acid esters can be used [11]. Irrespective of the ester used, the glycerol and carbonic acid esters are poorly miscible, since the former is a polar protic compound, and the latter is a polar nonprotic compound. Hence, the resulting mixture is a biphasic liquid–liquid system [13, 14]. Furthermore, in the presence of a heterogeneous catalyst, the complexity of the system increases to a triphasic liquid–liquid–solid system. Therefore, there are many operational difficulties that must be addressed from scientific and technological perspectives.

An important point is that the formation of glycerol carbonate by transesterification can involve parallel and in series reactions, forming co-products that contaminate the desired product [8, 15]. Although the identification of the chemical species formed is crucial to understand the process, most research on this transesterification process is not concerned with the formation of co products. In fact, even for the most studied reaction, between glycerol and dimethyl carbonate, there is no agreement in the literature about which chemical species can be formed [13, 16, 17].

Another fact that should be highlighted is that the catalyst selection represents an important point in the viability of the process. The catalyst properties define the reaction mechanism and can reduce or increase the products of the process. Transesterification reactions are promoted by catalysts with basic properties, with homogeneous catalysis being more widely used industrially, rather than heterogeneous catalysis [18]. More specifically, catalysts such as CH_3ONa, CH_3OK, Na_2CO_3, metallic oxides (CaO, MgO, ZnO and NiO) and even lipase are widely studied in the literature. However, CH_3ONa is the more commonly used in the

biodiesel industries, since it is very active, inexpensive and do not form soap emulsions [18–23]. Nevertheless, on a laboratory scale, various types of catalysts have been tested for the production of glycerol carbonate by transesterification, including acid catalysts that are inefficient in transesterification reactions [11, 16]. Notably, the use of hybrid organic–inorganic catalysts with basic properties could be advantageous to produce glycerol carbonate, especially since these materials can be synthesized using a range of procedures [24–28].

Therefore, the aim of this work was to investigate the reactions between glycerol and different carbonic acid esters (dimethyl carbonate, diethyl carbonate, ethylene carbonate and propylene carbonate), using CTA-MCM-41 hybrid silica as basic catalyst. To understand the process from a molecular catalysis perspective, all chemical species produced during the reactions were identified. Reaction steps and reaction mechanisms were proposed for these reactions, together with determination of the conditions to produce glycerol carbonate with maximum efficiency in terms of conversion, selectivity, and yield.

Materials and methods

Materials

Cetyltrimethylammonium bromide (CTAB, 98.0%), ammonium hydroxide solution (NH_3, 28.0–30.0%), tetraethyl orthosilicate (TEOS, 98.0%), 1,2,3-propanetriol (glycerol, GLY, 99.0%), dimethyl carbonate (DMC, 99.0%), diethyl carbonate (DEC, 99.0%), 1,3-dioxolan-2-one (ethylene carbonate, ECARB, 98.0%), 4-methyl-1,3-dioxolan-2-one (propylene carbonate, PCARB, 99.7%), dimethylformamide (DMF, 99.8%), methanol (CH_3OH, MeOH, 99.9%), 4-hydroxymethyl-1,3-dioxolan-2-one (glycerol carbonate, GCARB, 99.0%), and 2,3-epoxy-1-propanol (glycidol, GLYC, 96.0%) were obtained from Sigma-Aldrich (Merck).

Catalyst synthesis

The catalyst was synthesized according to the methodology described by Araújo et al. [29], using a reaction mixture with the following molar composition: 1 SiO_2: 12.5 NH_3: 0.4 CTAB: 174 H_2O: 4 EtOH. The synthesis was performed in a jacketed batch reactor, under autogenous pressure, with magnetic stirring at ~ 700 rpm and constant temperature of 30 °C. Firstly, the CTAB was dissolved in distilled water, with addition of NH_4OH solution in the proportion shown above, and the mixture was kept under stirring for 15 min. Tetraethyl orthosilicate (TEOS) was then added dropwise and the mixture was stirred for 2 h. In the next step, the reaction mixture with pH ~ 11 was filtered, and the solid material obtained was washed with distilled water until reaching pH ~ 9. The final solid was dried for 24 h in an oven at 60 °C, for use in the characterization analyses and the catalytic tests.

Characterization of the catalyst

The structure of the catalyst was analyzed by X-ray diffraction (XRD), using a Rigaku Multiflex diffractometer operating with Cu K_α radiation ($\lambda = 0.15418$ nm), voltage of 40 kV, current of 40 mA, goniometer speed of 2.0° min^{-1}, 2θ angle from 1.0° to 10.0°, and step size of 0.01°. The use of Bragg's law (Eq. 1) then enabled determination of the interplanar distances (Eq. 2) and confirmation of formation of the MCM-41 structure.

$$n\lambda = 2d \sin(\theta)_{hkl} \tag{1}$$

$$d_{hkl} = \frac{0.15418}{2 \sin(\theta)_{hkl}} \tag{2}$$

Thermogravimetric analysis (TGA) was used to quantify the mass loss of the organic material occluded within the mesopores of the catalyst, employing a TA Instruments SDT-Q600 analyzer. A mass of 10 mg of sample was weighed into an alumina crucible, followed by heating from ambient temperature to 850 °C, at a rate of 10 °C min^{-1}, under an oxidizing atmosphere provided by a flow of synthetic air at 40 mL min^{-1}. The organic material mass loss was used to calculate the mols of CTA^+ cations present in the catalyst (Eq. 3), enabling estimation of the number of basic sites per g of catalyst.

$$n_{sites} = n_{CTA^+} = \frac{\left(\frac{R_{II}+R_{III}}{100}\right)}{MM_{CTA^+}} \tag{3}$$

In Eq. 3, n_{CTA^+} is the number of mols of the CTA^+ cation present in the catalyst (mol g^{-1}), R_{II} and R_{III} are the percentage losses of organic material from the catalyst, obtained by thermogravimetry (%), and MM_{CTA^+} is the molar mass of the CTA^+ cation (g mol^{-1}).

Scanning electron microscopy (SEM) was used to obtain images of the CTA-MCM-41 hybrid silica particles. The analysis was performed on a FEI Company microscope model Magellan 400L, operated at 25 kV. The silica was dispersed in methanol, approximately 10 mg in 2 mL of methanol, and sonicated for 5 min. Drops of the dispersion were then deposited onto an aluminum sample holder, and once dried, the sample was covered with gold and analyzed. In previous studies, the CTA-MCM-41 catalyst was characterized by nitrogen physisorption, ^{29}Si MAS-NMR and by O 1s XPS to evaluate the catalyst porosity and the origin and strength of the basic sites, siloxy sites (SiO^-). [25, 30, 31].

Catalytic evaluation

The transesterification reactions of glycerol (GLY) with different carbonic acid esters (CAE) to produce glycerol carbonate (GCARB), Fig. S1, were conducted in

the presence of dimethylformamide (DMF), a polar nonprotic solvent. The procedures consisted of adaptations of methods described elsewhere [32, 33].

The catalytic tests were performed using a jacketed batch reactor with capacity of 35 mL, made of glass, under atmospheric pressure and magnetic stirring (approximately 0.1 MPa and 1500 rpm). For vapor recovery, a condenser, made of glass, maintained at around 20 °C was connected to the upper part of the reactor. The reactor was loaded with suitable amounts of the reactants (CAE and GLY, Fig. S1) to obtain a reaction mixture with the desired CAE:GLY molar ratio, diluted in DMF at a proportion of 50 wt%. The mixture of reactants and solvent was then heated to the desired temperature, under constant stirring. After reaching the operating temperature, the required amount of catalyst, calculated based only on the mass of the reactant mixture (CAE + GLY), was added to initiate the reaction.

The transesterification reactions were performed varying several parameters (temperature, percentage of catalyst and molar ratio of the reactants), as follows in Table 1.

The reactions were continued for up to 120 min, with 0.5 mL aliquots periodically removed from the reactor using a 1 mL syringe, with immediate separation from the catalyst, prior to chromatographic analysis. The separation was performed by attaching a microfilter containing a polytetrafluoroethylene (PFTE) membrane (Millex-LG, 0.20 µm, 13 mm diameter) to the syringe. All the evaluations were performed in triplicate, in order to estimate the deviation of the results. Furthermore, in order to test the stability of the catalyst, it was reused four times in the RDM reaction, using the following reaction conditions: 80 °C; 4 wt% catalyst; 2 DMC:1 GLY molar ratio and 60 min of reaction. After each reaction cycle, the catalyst was filtered, washed with methanol, dried in an oven at 80 °C for 3 h and reused for the next reaction cycle.

Analysis of the reaction products

Quantitative analysis of the samples removed during the reactions was performed using a gas chromatograph (GC-2010, Shimadzu, Tokyo, Japan) equipped

Table 1 Reaction conditions, chosen depending on the reactivity of the system

Reaction	Reaction parameters			
	Temperature (°C)	Catalyst (%)	Molar ratio (CAE/GLY)	Time (min)
RDM[a]	40; 60 or 80	1; 2 or 4	1; 2 or 3	120
RDE[b]	80	1	2	120
REC[c]	30; 50; 70 or 80	1	1 or 2	60 or 120
RPC[d]	80	1	2	120

[a]CAE = DMC

[b]CAE = DEC

[c]CAE = ECARB

[d]CAE = PCARB

with a flame ionization detector (FID) and a Restek RTX-WAX capillary column (30 m × 0.32 mm × 0.25 µm). Aliquots of around 1.0 µL of the samples were injected in split mode, with a split ratio of 50:1. The injector and detector temperatures were 260 and 280 °C, respectively. The carrier gas was high purity helium, at a flow rate of 2.62 mL min^{-1}. The optimized column temperature program for separation of the components was as follows: initial 50 °C for 1 min; ramp to 60 °C at 10 °C min^{-1}; hold at 60 °C for 2 min; ramp to 240 °C at 15 °C min^{-1}; hold at 240 °C until the end of the analysis. Calculations of the conversions, selectivities, and yields of the reactions were performed by the external standards method, using calibration curves for glycerol (GLY), glycerol carbonate (GCARB), and glycidol (GLYC). The equations are provided in the Supplementary Material. The other chemical species formed (glycerol monocarbonates, glycerol tricarbonate, and glycidol carbonate) were not quantified, due to the unavailability of commercial analytical standards.

In order to identify the reaction products, the samples were also analyzed qualitatively by gas chromatography coupled to mass spectrometry, using a GCMS-QP2010 Plus instrument (Shimadzu, Tokyo, Japan) fitted with a SUPELCOWAX® 10 Capillary GC Column (30 m × 0.25 mm × 0.25 µm). The column temperature program was similar to that used in the quantitative analyses (GC-FID). The ion source and spectrometer interface temperatures were 280 and 200 °C, respectively.

Results and discussion

Characterization of the catalyst

The diffractogram of the hybrid silica synthesized according to the methodology described by Araújo et al. [29] confirmed that it presented the typical MCM-41 structure (Fig. S2) [34–37]. The micrograph of the hybrid silica, Fig. S3, shows that the sample consisted of an agglomeration of particles with variable size, in the range of 1–5 µm, and undefined shape. The observed morphology was one of many that MCM-41 silica can present [29, 31, 38].

Fig. S4 shows the results of TGA of the as-synthesized silica heated in an oxidizing atmosphere, revealing four distinct mass loss regions. According to Zhao et al. [39], these regions were associated with the following events: (I) desorption of water adsorbed on the surface of the catalyst; (II) Hoffmann elimination of the organic cation (CTA^+); (III) combustion of residual organic matter; and (IV) dehydroxylation of silanol groups. The percentage mass losses in each region are shown in Table S6. The number of mols of cations present in the hybrid silica was calculated considering the organic matter percentages obtained for regions (II) and (III) (Eq. 3). Since each CTA^+ cation compensated a siloxy anion (SiO^-), it was considered that the total number of mols of catalytic sites present in the silica was equal to the number of mols of CTA^+ cations (Eq. 4).

$$n_{sites} = n_{SiO^-} = n_{CTA+} = 1.822 \text{ mmol } g^{-1} \quad (4)$$

Finally, in order to provide a better understanding of the catalyst properties, it should be highlighted that the pores of CTA-MCM-41 hybrid silica are obstructed by the CTA^+ micelles, and that the basic catalytic sites, siloxy anions SiO^-, are part of the inorganic exoskeleton of the hybrid silica. As reported in the literature, ^{29}Si MAS-NMR and O 1s XPS analyzes proved that the silica has strong basic sites and nitrogen physisorption shows that it has a very low surface area (1.0–4.1 $m^2\ g^{-1}$) [25, 40, 41]. Therefore, any reaction performed using this catalyst must occur on its outer surface. Hence, there is no internal diffusion of the reactants and products, and the catalytic sites located within the mesopores are not accessible to the reactants.

Catalytic evaluation

Transesterification between glycerol and dimethyl carbonate

Fig. 1a shows the effect of the reaction system temperature on the conversion of glycerol (GLY), for an initial reactants ratio (DMC:GLY) of 2:1. At all the temperatures studied, there was an initial very rapid consumption of glycerol, followed by a slower rate after several minutes. Interestingly, the initial selectivity towards glycerol carbonate (GCARB) was very low (Fig. 1b), indicating that it was not a primary product. Kumar et al. [32] observed similar behavior for the glycerol consumption rate, using hydrotalcite and hydromagnesite as catalysts, without formation of glycerol carbonate, which was attributed to strong adsorption of glycerol on the catalyst. It can also be seen from Fig. 1a that increase of the temperature led to an increase in the rate of glycerol consumption, with conversions of 49, 58, and 75% obtained after 120 min of reaction at temperatures of 40, 60, and 80 °C.

Fig. 1b shows the selectivity towards the two main products of the reaction. It can be seen that the selectivity towards glycerol carbonate (GCARB) was initially low, at all the temperatures studied, followed by an increase. The mass spectroscopy (GC–MS) analysis (Fig. S5) enabled the identification of two products whose molecular masses corresponded to glycerol monocarbonates. Two parallel reactions

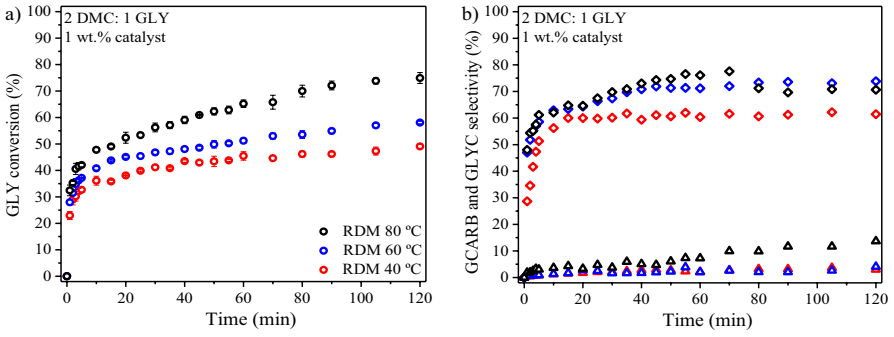

Fig. 1 Effect of temperature on RDM reaction: **a** glycerol conversion (circle) and **b** glycerol carbonate selectivity (diamond) and glycidol selectivity (triangle). Reaction conditions: 2 DMC: 1 GLY and 1 wt% catalyst

(R1 and R2) resulted in the formation of these two primary products (glycerol monocarbonates, isomers P1 and P2). These two primary products could then undergo cyclization reactions (R3 and R4), forming glycerol dicarbonate (commonly known as glycerol carbonate) as the secondary product S1 (Fig. 2). Although the formation of the two primary products has been proposed in several previous studies [13, 15, 33], none of them succeeded in identifying these molecules, due to the speed with which they were consumed. It can also be seen from Fig. 1b that at 40 °C, the selectivity towards glycerol carbonate was constant (60%) after 10 min, while at 60 °C, the selectivity towards glycerol carbonate was constant (72%) after 45 min of reaction. At 80 °C, maximum selectivity towards glycerol carbonate (78%) was obtained after 70 min, followed by a subsequent decrease to 70%.

In parallel with the decrease in selectivity towards glycerol carbonate observed at 80 °C, two tertiary products were formed, namely glycidol (GLYC, T1) and glycerol tricarbonate (T2), according to reactions R5 and R6 (Fig. 2). Reaction R5 involved the decomposition of glycerol carbonate to produce glycidol and carbon dioxide, while reaction R6 was due to another transesterification between dimethyl carbonate and the hydroxyl in glycerol carbonate.

The results for glycidol formation (Fig. 1b) showed that when the reaction was performed at lower temperatures (40 and 60 °C), the selectivity towards this product was low, at around 3% after 120 min of reaction. However, at 80 °C, the production of glycidol was more important, especially after 60 min, with 14% selectivity after 120 min. As noted above, in parallel with the increased selectivity towards glycidol, there was a decrease in selectivity towards glycerol carbonate, due to reaction R5. The formation of glycidol as a reaction product was reported by Gade et al. [42], but was contested by Bai et al. [17]. The present results confirmed that the decomposition of glycerol carbonate to glycidol is, in fact, one of the reaction steps. Additional information has been provided in the Supplementary Material (Figs. S5, S6).

The use of gas chromatography coupled with mass spectroscopy enabled identification of the presence of glycerol tricarbonate. As described previously, this tertiary product (T2) was probably formed by the transesterification reaction of glycerol carbonate with dimethyl carbonate. It was not possible to quantify the formation of glycerol tricarbonate, although it was evident that it was present at a very low concentration, as indicated by the small size of the chromatographic peak corresponding to this product. Rokicki et al. [8] also detected the formation of glycerol tricarbonate (T2) under specific conditions using a large excess of dimethyl carbonate, with DMC:GLY ratios greater than 5:1. However, the present results demonstrated that reaction R6 could occur even using lower DMC:GLY ratios.

Fig. 3 shows the effect of the mass percentage of catalyst fed to the reaction system on glycerol conversion and selectivity towards the two main products. Increase of the catalyst mass acted to increase glycerol conversion, with values after 120 min of 75, 86, and 90% obtained using 1, 2, and 4 wt% catalyst (Fig. 3a), as expected due to the greater quantity of available catalytic sites. Increase of the catalyst concentration led to lower selectivity towards glycerol carbonate and higher selectivity towards glycidol, with the latter compound becoming the second main product of the process. When 2 wt% catalyst was used, there was a gradual decrease in the selectivity towards glycerol carbonate and an increase in the selectivity towards

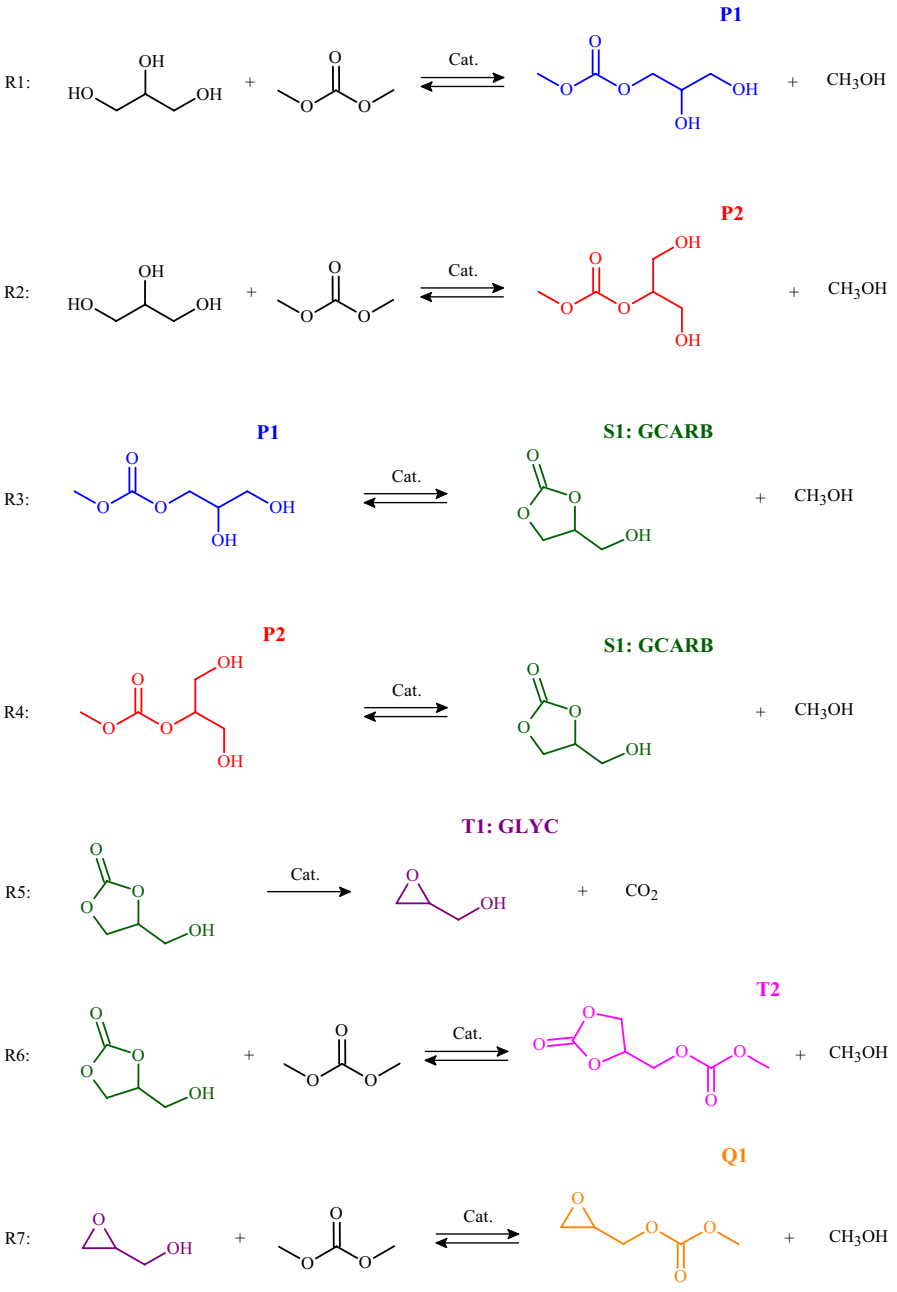

Fig. 2 Reaction steps of the transesterification between glycerol and dimethyl carbonate

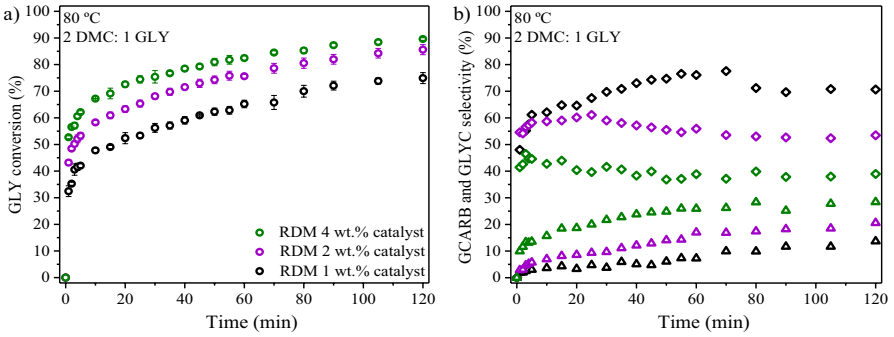

Fig. 3 Effect of catalyst loading on RDM reaction: **a** glycerol conversion (circle) and **b** glycerol carbonate selectivity (diamond) and glycidol selectivity (triangle). Reaction conditions: 80 °C and 2 DMC: 1 GLY

glycidol, reaching values of 52 and 21%, respectively, after 120 min. Similarly, in the presence of 4 wt% catalyst, the selectivities to glycerol carbonate and glycidol reached values of 38 and 28%, respectively, after 120 min.

Finally, the GC–MS analysis identified the presence of glycidol carbonate, formed in reaction R7 (Fig. 2). This quaternary product (Q1) was most evident when there was greater formation of glycidol, after 80 min in the reaction using 4 wt% catalyst. The formation of Q1, which was the last reaction step detected in the process, was accompanied by slight decreases in the selectivity towards glycidol (Fig. 3b) and the glycidol yield (Fig. S28). It should be highlighted that the formation of glycidol carbonate has not been reported in the literature. Although it was not quantified, the concentration of this product must have been very low, considering the small size of the chromatographic peak.

Fig. 4 shows the effect of the DMC:GLY molar ratio (i.e., excess dimethyl carbonate) on reaction performance. As expected, increase of the molar ratio increased

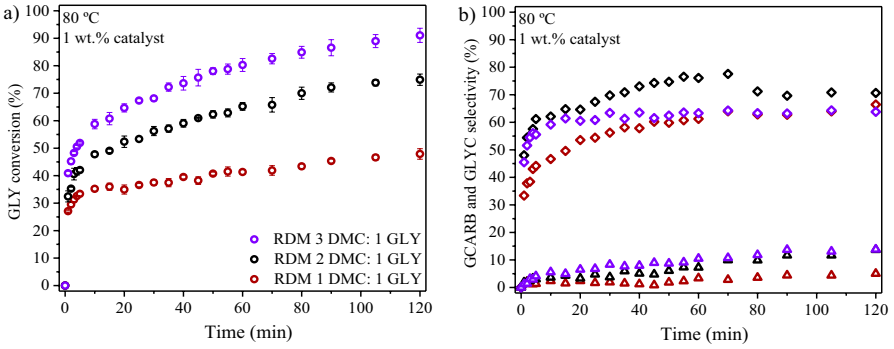

Fig. 4 Effect of DMC: GLY molar ratio on RDM reaction: **a** glycerol conversion (circle) and **b** glycerol carbonate selectivity (diamond) and glycidol selectivity (triangle). Reaction conditions: 80 °C and 1 wt% catalyst

glycerol conversion (Fig. 4a), since the excess of DMC shifted the reaction equilibrium, favoring formation of the products. Conversions of 48, 75, and 91% after 120 min were obtained using DMC/GLY = 1, 2, and 3.

Fig. 4b shows the influence of the DMC:GLY ratio on the selectivity towards the two main products. When the reaction was performed with an equimolar DMC:GLY ratio, the selectivity towards glycerol carbonate showed an increasing temporal trend. This confirmed that GCARB was a secondary product and that its formation was slower at the start of the reaction, due to lower conversion of glycerol monocarbonates to glycerol carbonate. As the reaction proceeded, the selectivity towards glycerol carbonate became constant, at 60%, and there was the initiation of formation of glycerol tricarbonate from the transesterification reaction between glycerol carbonate and dimethyl carbonate. Rokicki et al. [8] reported similar behavior using DMC:GLY ratios up to 10:1. As the excess of DMC in the system increased, more glycerol carbonate was consumed and greater quantities of glycerol tricarbonate were formed.

When the reaction was performed using a DMC:GLY ratio of 2:1, the selectivity towards GCARB increased, since the excess of DMC favored the conversion of glycerol to form the primary products P1 and P2, according to the fast reactions R1 and R2. Subsequently, as the process continued, the rates of reactions R5 and R6 increased, leading to lower selectivity towards glycerol carbonate, as explained above (Figs. 1, 2). When the reaction was performed with increase of the DMC:GLY molar ratio to 3:1, the initial selectivity towards glycerol carbonate increased very similarly to that observed using a DMC:GLY ratio of 2:1. However, after 15 min of reaction, the selectivity towards glycerol carbonate remained constant at 60%, as observed for the DMC:GLY ratio of 1:1, due to its consumption according to reaction R6, generating glycerol tricarbonate.

Finally, regarding the selectivity towards glycidol (Fig. 4b), when an equimolar ratio was used, the selectivity towards glycidol reached 5% after 120 min of reaction. When an excess of DMC was used (DMC:GLY = 2:1), the formation of glycidol was favored, since there was greater formation of glycerol carbonate, from which glycidol was formed, with 14% selectivity reached after 120 min of reaction. When the amount of DMC was increased further (DMC:GLY = 3:1), the glycidol selectivity became very similar to that obtained using the previous ratio (DMC:GLY = 2:1), reaching 15% after 120 min of reaction. This was because the formation of glycidol was independent of the dimethyl carbonate content. Rokicki et al. [8] reported that increase of the dimethyl carbonate content only acted to increase the transformation of glycerol carbonate to glycerol tricarbonate, with subsequent transformation of glycerol tricarbonate to diglycerol hexacarbonate.

Transesterification between glycerol and different esters

Fig. 5 shows the effect of the ester type on the conversion of glycerol. It can be seen from Fig. 5a that cyclic-chain esters (REC and RPC, Fig. S1) have a much higher reactivity than straight-chain esters (RDM and RDE, Fig. S1). It can also be seen that the increase in the alkyl chain of the ester, straight or cyclic, causes a reduction of its reactivity, either by inductive effect or by the increase of diffusional effects

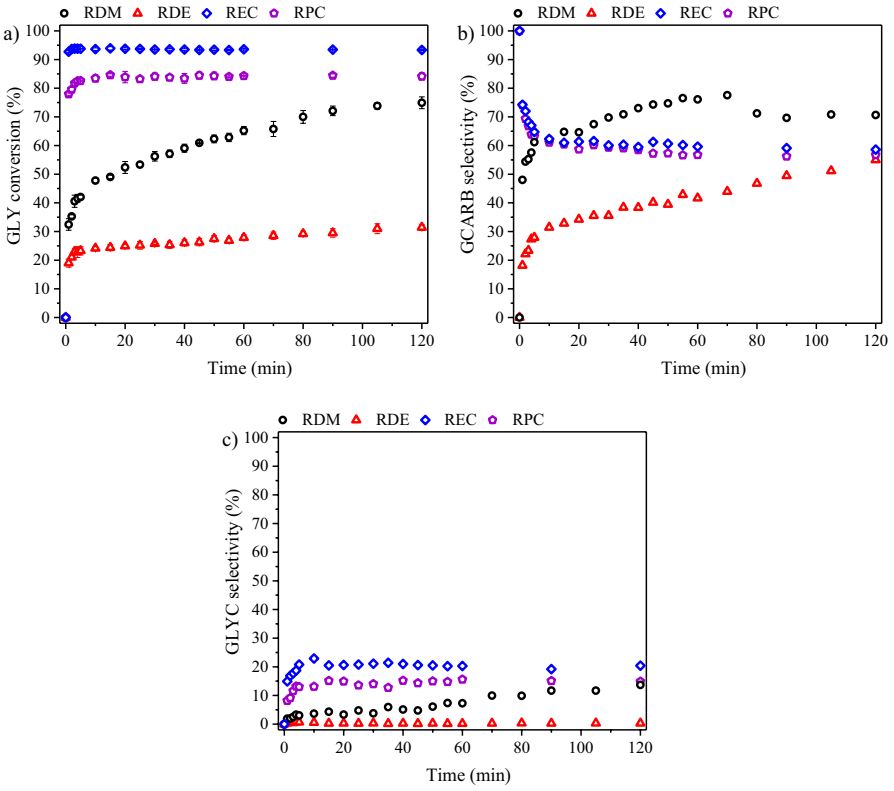

Fig. 5 Effect of carbonic acid ester type on **a** the conversion of glycerol to **b** glycerol carbonate selectivity, **c** glycol selectivity. RDM reaction (CAE = DMC); RDE reaction (CAE = DEC); REC reaction (CAE = ECARB) and RPC reaction (CAE = PCARB). Reaction conditions: 80 °C, 2 CAE: 1 GLY and 1 wt% catalyst

during the reaction on the surface of the catalyst [43]. Fig. 5a also shows that the reactions with ethylene carbonate and propylene carbonate (ECARB and PCARB, Fig. S1), both cyclic-chain esters, reached equilibrium after 5 min of reaction, with conversions of 94% and 83%, respectively. Reactions with dimethyl carbonate and diethyl carbonate (DMC and DEC, Fig. S1), both straight-chain esters, achieved much lower conversions, 75% and 31% after 120 min of reaction.

Fig. 5b shows the selectivity towards the formation of glycerol carbonate. It can be seen that for the cyclic-chain esters (REC and RPC) the selectivities towards this product tend to be 100% when the reaction starts. This behavior is typical for the formation of a primary product of a reaction, meaning, therefore, that the cyclic-chain esters are directly transformed into glycerol carbonate (reaction R1 in Fig. S22). As the reaction time increases, the selectivity towards glycerol carbonate decreases and, in parallel, the glycidol selectivity increases (Fig. 5c), suggesting that this last one is a secondary product, derived from glycerol carbonate (reaction R2 in Fig. S22). Fig. 5b also shows that the behavior of the selectivity towards glycerol carbonate for the straight-chain esters (RDM and RDE) is opposite to the cyclic-chain esters,

in other words, it tends to be 0% when the reaction starts. This behavior suggests that, in this case, glycerol carbonate is a secondary product, formed, therefore, from another intermediary product. In fact, analysis of the reaction products shows that straight-chain esters form glycerol monocarbonates (P1 and P2 in Figs. S5 and S21).

Interestingly, the production of glycidol as the main co-product of these reactions becomes interesting, since this molecule is industrially promising and can be used in several applications [44, 45], as well, short-chain alcohols, which are products of the reactions and can be reused in different chemical processes [46–49].

Based on the above discussions, two mechanisms have been proposed for the transesterification of glycerol with cyclic-chain and straight-chain esters, in the presence of a strong basic catalyst, Figs. S26 and 6.

According to Schuchardt et al. [50], the transesterification between an alcohol and an ester, in the presence of a basic catalyst, starts with the formation of an alkoxide. Therefore, according to Ochoa-Gómez et al. [33], the reaction between dimethyl carbonate and glycerol starts from the adsorption of glycerol at the basic site, generating a glyceroxide anion and the conjugated acid (BH) of the base (steps 1 and 2 in Fig. S26). Then, the glyceroxide anion attacks the carbonyl carbon of the

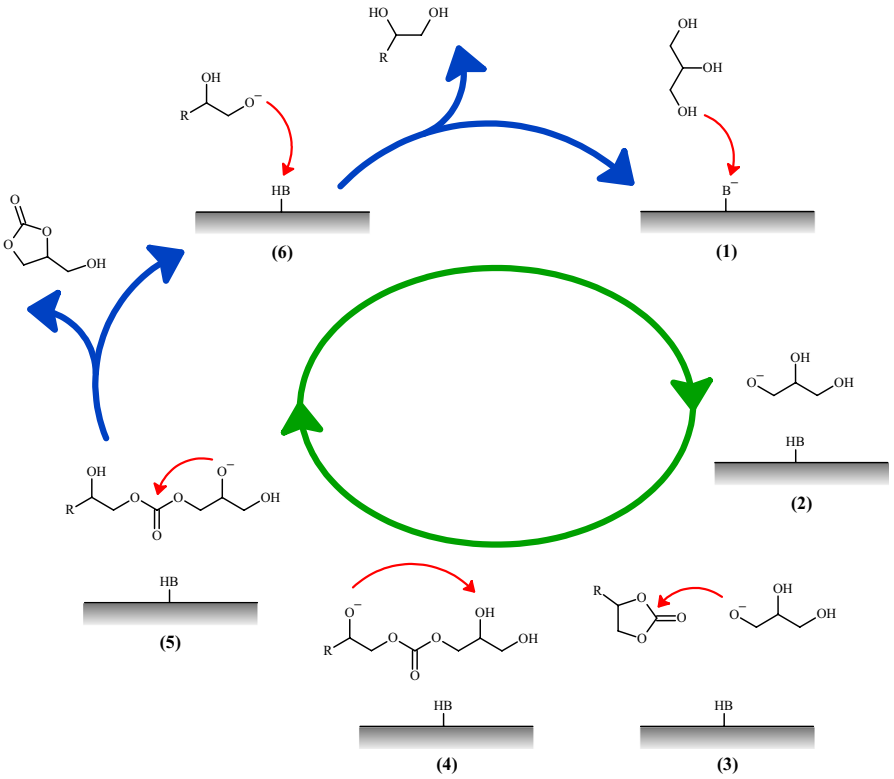

Fig. 6 Possible reaction mechanism for glycerol carbonate formation from transesterification of glycerol with cyclic-chain esters

ester (step 3), forming a glycerol monocarbonate as a primary product (step 4) and a methoxide anion that attacks the conjugated acid (BH), regenerating the basic site and forming a molecule of methanol. Finally, glycerol monocarbonate undergoes a cyclization reaction, without interacting with the catalyst, forming glycerol carbonate and one more methanol molecule. However, it should be highlighted that the glycerol monocarbonate can adsorb on the basic site (step 5) generating a glyceroxide monocarbonate anion and the conjugated acid BH (step 6). Finally, the glyceroxide monocarbonate anion undergoes cyclization, generating the glycerol carbonate and a methoxide anion that attacks the acid (BH), regenerating the basic site and forming methanol. This mechanism explains our results, aids in the understanding of previous work [32], and can be applied to all straight-chain esters.

Similarly, the transesterification using cyclic-chain esters starts from the adsorption of glycerol at the basic site, generating a glyceroxide anion and the conjugated acid (BH) of the base (Fig. 6, steps 1 and 2). Subsequently, the glyceroxide anion attacks the carbonyl carbon of the ester, generating a glyceroxide monocarbonate anion (steps 3 and 4). Then, the glyceroxide monocarbonate anion, through an attack on its second hydroxyl, forms a second glyceroxide monocarbonate anion (steps 4 and 5). Afterwards, this anion attacks the carbonyl carbon generating glycerol carbonate and alkoxide (steps 5 and 6). Finally, the alkoxide attacks the conjugated acid (BH), regenerating the basic site and forming a glycol molecule (step 6). Thus, through this proposed reaction mechanism, unlike the straight-chain esters (Fig. S26, step 4), glycerol monocarbonate is not formed as a stable molecule in the system and, therefore, glycerol carbonate is the primary product of these reactions.

Finally, based on the above discussions, two mechanisms were proposed for the formation of glycidol, glycerol tricarbonate and glycidol carbonate, in the presence of a strong basic catalyst, Figs. S31 and S32. Furthermore, it should be highlighted that catalyzed by CTA-MCM-41 hybrid silica, the RDM and REC reactions showed apparent activation energies with values of 1.24 kJ mol^{-1} and 6.75 kJ mol^{-1} ($R^2 > 0.99$), respectively. These results, obtained from the linearization of the Arrhenius equation (Fig. S23, related to Figs. 1 and S24), confirm the high reactivity of cyclic-chain ethylene carbonate, which presented a much lower activation energy than the straight-chain dimethyl carbonate. These very low activation energies results suggest that CTA-MCM-41 hybrid silica has very high catalytic activity, which is due to the very strong basicity of the siloxy sites. However, due to weak interaction between siloxy anions and the CTA^+ cations, the catalyst has a slow deactivation, due to partial CTA^+ leaching to the liquid medium during the transesterification reaction (Fig. S33).

Conclusions

This work investigated the reactions between glycerol and different carbonic acid esters, straight-chain esters and cyclic-chain esters, using CTA-MCM-41 hybrid silica as basic catalyst. CTA-MCM-41 hybrid silica, with particle size in the range of 1 to 5 μm and catalytic sites concentration of 1.822 mmol g^{-1}, presented high catalytic activity. In the presence of this strong basic catalyst, straight-chain esters

and cyclic-chain esters formed glycerol carbonate following different reaction mechanisms.

Among all the esters, ethylene carbonate and dimethyl carbonate showed higher reactivity and their reactions showed apparent activation energies with values of 1.24 kJ mol^{-1} and 6.75 kJ mol^{-1}, respectively. Straight-chain esters formed six products: two isomers of glycerol monocarbonate as primary products, glycerol carbonate as secondary product, glycidol and glycerol tricarbonate as tertiary products and glycidol carbonate as a quaternary product. On the other hand, cyclic-chain esters formed four products: glycerol carbonate as primary product, glycidol and glycerol tricarbonate as secondary products and glycidol carbonate as tertiary product.

The formation of co-products, glycidol carbonate and glycerol tricarbonate, is reduced when a small excess of ester is used, and the reactions are conducted for short reaction times. Glycerol carbonate was produced most efficiently under mild reaction conditions, while maximum glycidol production was achieved when a higher loading of catalyst was used in the reaction system.

Supplementary Information The online version contains supplementary material available at https://doi.org/10.1007/s11144-023-02349-4.

Acknowledgements The authors are grateful for the financial support provided by the following Brazilian agencies: Conselho Nacional de Desenvolvimento Científico e Tecnológico (CNPq, Grant #141307/2018-8) and Coordenação de Aperfeiçoamento de Pessoal de Nível Superior (CAPES).

References

1. Abomohra AEF, Elsayed M, Esakkimuthu S et al (2020) Potential of fat, oil and grease (FOG) for biodiesel production: a critical review on the recent progress and future perspectives. Prog Energy Combust Sci 81:100868. https://doi.org/10.1016/j.pecs.2020.100868
2. De Lima AL, Ronconi CM, Mota CJA (2016) Heterogeneous basic catalysts for biodiesel production. Catal Sci Technol 6:2877–2891. https://doi.org/10.1039/c5cy01989c
3. Singh D, Sharma D, Soni SL et al (2020) A review on feedstocks, production processes, and yield for different generations of biodiesel. Fuel 262:116553. https://doi.org/10.1016/j.fuel.2019.116553
4. ANP (2022) Oil, natural gas and biofuels statistical yearbook 2022. http://bit.ly/3wsTFTC
5. da Silva LD, Santos RC, Silva JGAB et al (2022) Direct ammoxidation of glycerol to nitriles using Mo/alumina catalysts. Reac Kinet Mech Cat 135:271–285. https://doi.org/10.1007/s11144-021-02111-8
6. Wang A, Xu Q, Yin H (2022) Synthesis of lactic acid starting from glycerol catalyzed by CaO-supported CuO and metallic Cu catalysts in $Ca(OH)_2$ aqueous solution. Reac Kinet Mech Cat. https://doi.org/10.1007/S11144-022-02328-1
7. Eisenhart AE, Beck TL (2021) Quantum simulations of hydrogen bonding effects in glycerol carbonate electrolyte solutions. J Phys Chem B 125:2157–2166. https://doi.org/10.1021/acs.jpcb.0c10942
8. Rokicki G, Rakoczy P, Parzuchowski P, Sobiecki M (2005) Hyperbranched aliphatic polyethers obtained from environmentally benign monomer: glycerol carbonate. Green Chem 7:529–539. https://doi.org/10.1039/b501597a
9. Szori M, Giri BR, Wang Z et al (2018) Glycerol carbonate as a fuel additive for a sustainable future. Sustain Energy Fuels 2:2171–2178. https://doi.org/10.1039/c8se00207j
10. Hu C, Yoshida M, Chen HC et al (2021) Production of glycerol carbonate from carboxylation of glycerol with CO_2 using ZIF-67 as a catalyst. Chem Eng Sci 235:116451. https://doi.org/10.1016/j.ces.2021.116451

11. Sonnati MO, Amigoni S, Darmanin T, Choulet O (2013) Glycerol carbonate as a versatile building block for tomorrow: synthesis, reactivity, properties and applications. Green Chem 15:283–306. https://doi.org/10.1039/c2gc36525a
12. Sahani S, Upadhyay SN, Sharma YC (2021) Critical review on production of glycerol carbonate from byproduct glycerol through transesterification. Ind Eng Chem Res 60:67–88. https://doi.org/10.1021/acs.iecr.0c05011
13. Esteban J, Domínguez E, Ladero M, Garcia-Ochoa F (2015) Kinetics of the production of glycerol carbonate by transesterification of glycerol with dimethyl and ethylene carbonate using potassium methoxide, a highly active catalyst. Fuel Process Technol 138:243–251. https://doi.org/10.1016/j.fuproc.2015.06.012
14. Esteban J, Fuente E, Blanco A et al (2015) Phenomenological kinetic model of the synthesis of glycerol carbonate assisted by focused beam reflectance measurements. Chem Eng J 260:434–443. https://doi.org/10.1016/j.cej.2014.09.039
15. Kim SC, Kim YH, Lee H et al (2007) Lipase-catalyzed synthesis of glycerol carbonate from renewable glycerol and dimethyl carbonate through transesterification. J Mol Catal B 49:75–78. https://doi.org/10.1016/j.molcatb.2007.08.007
16. Zhu J, Chen D, Wang Z et al (2022) Synthesis of glycerol carbonate from glycerol and dimethyl carbonate over CaO-SBA-15 catalyst. Chem Eng Sci 258:117760. https://doi.org/10.1016/j.ces.2022.117760
17. Bai R, Zhang H, Mei F et al (2016) Retraction: one-pot synthesis of glycidol from glycerol and dimethyl carbonate over a highly efficient and easily available solid catalyst $NaAlO_2$ (Green Chemistry (2013) 15 (2929–2934) https://doi.org/10.1039/C3GC40855H). Green Chem 18:6144. https://doi.org/10.1039/c6gc90102f
18. Helwani Z, Othman MR, Aziz N et al (2009) Solid heterogeneous catalysts for transesterification of triglycerides with methanol: a review. Appl Catal A 363:1–10. https://doi.org/10.1016/j.apcata.2009.05.021
19. Zhang Y, Niu S, Han K et al (2021) Synthesis of the SrO–CaO–Al_2O_3 trimetallic oxide catalyst for transesterification to produce biodiesel. Renew Energy 168:981–990. https://doi.org/10.1016/j.renene.2020.12.132
20. Sulaiman NF, Ramly NI, Abd Mubin MH, Lee SL (2021) Transition metal oxide (NiO, CuO, ZnO)-doped calcium oxide catalysts derived from eggshells for the transesterification of refined waste cooking oil. RSC Adv 11:21781–21795. https://doi.org/10.1039/d1ra02076e
21. Miladinović MR, Krstić JB, Zdujić MV et al (2022) Transesterification of used cooking sunflower oil catalyzed by hazelnut shell ash. Renew Energy 183:103–113. https://doi.org/10.1016/j.renene.2021.10.071
22. Chen HX, Xia W, Wang S (2022) Biodiesel production from waste cooking oil using a waste diaper derived heterogeneous magnetic catalyst. Braz J Chem Eng. https://doi.org/10.1007/s43153-022-00257-z
23. Wu S, Wu Y, Sun B et al (2022) Experimental and optimization for kinetic resolution of 1-(4-(trifluoromethyl)phenyl)ethanol enantiomers by lipase-catalyzed transesterification in organic phase. Reac Kinet Mech Cat. https://doi.org/10.1007/s11144-022-02339-y
24. Eid JG, de Paula GM, Cardoso D (2022) Heterogeneous transesterification catalyzed by silicas containing basic sites. Mol Catal 531:112631. https://doi.org/10.1016/j.mcat.2022.112631
25. Martins L, Bonagamba TJ, de Azevedo ER et al (2006) Surfactant containing Si-MCM-41: an efficient basic catalyst for the Knoevenagel condensation. Appl Catal A 312:77–85. https://doi.org/10.1016/j.apcata.2006.06.035
26. Zapelini IW, Cardoso D (2021) Amine-grafted Na-LTA zeolite precursors as basic catalysts for Knoevenagel condensation. Microporous Mesoporous Mater 324:111270. https://doi.org/10.1016/j.micromeso.2021.111270
27. Wang Y, He R, Wang C, Li G (2021) Ionic liquids supported at MCM-41 for catalyzing CO_2 into cyclic carbonates without co-catalyst. Reac Kinet Mech Cat 134:823–835. https://doi.org/10.1007/s11144-021-02097-3
28. Rath D, Rana S, Parida KM (2014) Organic amine-functionalized silica-based mesoporous materials: an update of syntheses and catalytic applications. RSC Adv 4:57111–57124. https://doi.org/10.1039/c4ra08005j
29. Araújo JA, Cruz FT, Cruz IH, Cardoso D (2013) Encapsulation of polymers in CTA-MCM-41 via microemulsion. Microporous Mesoporous Mater 180:14–21. https://doi.org/10.1016/j.micromeso.2013.05.010

30. Fabiano DP, Hamad B, Cardoso D, Essayem N (2010) On the understanding of the remarkable activity of template-containing mesoporous molecular sieves in the transesterification of rapeseed oil with ethanol. J Catal 276:190–196. https://doi.org/10.1016/J.JCAT.2010.09.015
31. Silva LL, Alkimim IP, Costa JPVS et al (2019) Catalytic evaluation of MCM-41 hybrid silicas in the transesterification reactions. Microporous Mesoporous Mater 284:265–275. https://doi.org/10.1016/j.micromeso.2019.04.024
32. Kumar A, Iwatani K, Nishimura S et al (2012) Promotion effect of coexistent hydromagnesite in a highly active solid base hydrotalcite catalyst for transesterifications of glycols into cyclic carbonates. Catal Today 185:241–246. https://doi.org/10.1016/j.cattod.2011.08.016
33. Ochoa-Gómez JR, Gómez-Jiménez-Aberasturi O, Maestro-Madurga B et al (2009) Synthesis of glycerol carbonate from glycerol and dimethyl carbonate by transesterification: catalyst screening and reaction optimization. Appl Catal A 366:315–324. https://doi.org/10.1016/j.apcata.2009.07.020
34. de Paula LNR, de Paula GM, Rodrigues MGF (2020) Adsorption of reactive blue BF-5G dye on MCM-41 synthesized from chocolate clay. Ceramica 66:269–276. https://doi.org/10.1590/0366-69132020663792862
35. Beck JS, Vartuli JC, Roth WJ et al (1992) A new family of mesoporous molecular sieves prepared with liquid crystal templates. J Am Chem Soc 114:10834–10843. https://doi.org/10.1021/ja00053a020
36. Cai Q, Lin W-Y, Xiao F-S et al (1999) The preparation of highly ordered MCM-41 with extremely low surfactant concentration. Microporous Mesoporous Mater 32:1–15. https://doi.org/10.1016/S1387-1811(99)00082-7
37. Khushalani D, Kuperman A, Coombs N, Ozin GA (1996) Mixed surfactant assemblies in the synthesis of mesoporous silicas. Chem Mater 8:2188–2193. https://doi.org/10.1021/cm9600945
38. Medeiros de Paula G, do Nascimento Rocha de Paula L, Freire Rodrigues MG (2022) Production of MCM-41 and SBA-15 hybrid silicas from industrial waste. Silicon 14:439–447. https://doi.org/10.1007/S12633-020-00831-5
39. Zhao XS, Lu GQ, Whittaker AK et al (1997) Comprehensive study of surface chemistry of MCM-41 using ^{29}Si CP/MAS NMR, FTIR, pyridine-TPD, and TGA. J Phys Chem B 101:6525–6531. https://doi.org/10.1021/jp971366+
40. Silva LL, Alkimim IP, Vasquez PAS, Cardoso D (2017) Synthesis and properties of MCM-41 with polymerizable CADMA cationic surfactant. Catal Today 289:2–13. https://doi.org/10.1016/j.cattod.2016.06.041
41. Kubota Y, Nishizaki Y, Ikeya H et al (2004) Organic-silicate hybrid catalysts based on various defined structures for Knoevenagel condensation. Microporous Mesoporous Mater 70:135–149. https://doi.org/10.1016/j.micromeso.2004.02.017
42. Gade SM, Munshi MK, Chherawalla BM et al (2012) Synthesis of glycidol from glycerol and dimethyl carbonate using ionic liquid as a catalyst. Catal Commun 27:184–188. https://doi.org/10.1016/j.catcom.2012.07.003
43. de Paula LNR, de Paula GM, Cardoso D (2022) Kinetic study of ethyl esters transesterification using hybrid silica as catalyst. Reac Kinet Mech Cat 135:2427–2439. https://doi.org/10.1007/s11144-022-02258-y
44. Luo Q, Zeng M, Wang X et al (2020) Glycidol-functionalized macroporous polymer for boron removal from aqueous solution. React Funct Polym 150:104543. https://doi.org/10.1016/j.reactfunctpolym.2020.104543
45. Ricciardi M, Cespi D, Celentano M et al (2017) Bio-propylene glycol as value-added product from Epicerol® process. Sustain Chem Pharm 6:10–13. https://doi.org/10.1016/j.scp.2017.06.003
46. Tian P, Wei Y, Ye M, Liu Z (2015) Methanol to olefins (MTO): from fundamentals to commercialization. ACS Catal 5:1922–1938. https://doi.org/10.1021/acscatal.5b00007
47. Yue H, Zhao Y, Ma X, Gong J (2012) Ethylene glycol: properties, synthesis, and applications. Chem Soc Rev 41:4218–4244. https://doi.org/10.1039/c2cs15359a
48. Zhang M, Yu Y (2013) Dehydration of ethanol to ethylene. Ind Eng Chem Res 52:9505–9514. https://doi.org/10.1021/ie401157c
49. Jiménez RX, Young AF, Fernandes HLS (2020) Propylene glycol from glycerol: process evaluation and break-even price determination. Renew Energy 158:181–191. https://doi.org/10.1016/j.renene.2020.05.126

50. Schuchardt U, Sercheli R, Vargas RM (1998) Transesterification of vegetable oils: a review. J Braz Chem Soc 9:199–210. https://doi.org/10.1590/S0103-50531998000300002